doi.org/10.36721/PJPS.2020.33.4.SUP.1823-1832.1

Rutin coated gold nanoparticles prevent rhabdomyolysis-induced kidney injury via down-regulation of NF-kB, iNOS, IL-6 and up-regulation of HO-1 and Kim-1 genes in mice

Nadia Saifulah[1], Rehan Ahmed Siddiqui[2*], Muhammad Owais Ismail[1], Zahida Memon[1], Zara Aslam[3] and Muhammad Raza Shah[3]

[1]Department of Pharmacology, Ziauddin Medical College, Ziauddin University, Karachi, Pakistan
[2]Department of Research, Ziauddin University, Karachi, Pakistan
[3]HEJ Research Institute of Chemistry, International Center for Chemical and Biological Sciences, University of Karachi, Karachi

Abstract: The aim of this study was to evaluate the protective activity of rutin, and its gold nanoparticles (Ru-AuNPs) in rhabdomyolysis-induced acute kidney injury (AKI) model in mice. Rutin (25 and 50 mg/kg) and Ru-AuNPs (15 and 25 mg/kg) were administered to the animals for four (4) days with water deprivation for 24 hours followed by 50% glycerol injection at the dose of 10 ml/kg *intramuscularly*. On the next day, animals were dissected and blood and kidneys were collected. Biochemical investigations were performed to evaluate kidney functions, histological studies were carried out to see the changes at tissue level and real-time RT-PCR studies for nuclear factor-κB p50, NFκB; inducible nitric oxide synthase, iNOS; heme oxygenase-1, HO-1; interleukin-6, IL-6; and kidney injury molecule-1, Kim-1 were performed to elucidate the molecular mechanisms. Blood urea and creatinine were found to be decreased in animals treated with rutin and Ru-AuNPs. Down regulation of the mRNA expressions of iNOS, IL-6 and NFkB p50 and up-regulation of Kim-1 and HO-1 genes were observed. The efficacy of Ru-AuNPs was better than rutin alone even at a dose far less than the compound. Rutin and Ru-AuNPs alleviates kidney injury and inflammation in rhabdomyolysis-induced AKI model via anti-inflammatory and anti-oxidant pathways which make it a plausible compound for future studies.

Keywords: Rutin, acute kidney injury, rhabdomyolysis, glycerol, gold nanoparticles.

INTRODUCTION

Acute kidney injury (AKI) has the highest fatality rates of any diseases around the globe. It can be caused by ischemia, drugs, inflammation, or renal obstruction (Makris and Spanou, 2016). Rhabdomyolysis is one of the significant root of AKI, which has the 50% prevalence rate among all cases of AKI and has 5-10% mortality rate which has not changed for many years (Petejova *et al*., 2018). In rhabdomyolysis, free hemoglobin and myoglobin are accumulated in the kidneys where it induces lipid peroxidation of renal proximal tubular cells leading to inflammatory cascades activation (Manis *et al*., 2019). Currently, specific treatment of AKI is available except for supportive therapy or kidney transplant if kidney function is completely lost (Kher *et al*., 2017). Recent scientific studies, however, has found several compounds and extracts such as diacerein (Abd-Ellatif *et al*., 2019), N-acetylcysteine (Cui *et al*., 2019), L-carnitine (Gao *et al*., 2017), suramin (El-Kordy, 2019) and ascorbic acid (Ozturk *et al*., 2017; Li *et al*., 2011) that may aid in potential clinical trials to treat AKI. There is still a great need to explore new therapeutic compounds for the prevention of kidney injury.

A murine model of AKI caused by rhabdomyolysis is created by *intra-muscular* administration of 50% glycerol that massively damages skeletal muscles. As a result, free myoglobin circulates in the blood and deposited in the kidney where it causes renal obstruction, oxidative damage, inflammation and necrosis which in turns lead to AKI (Korrapati *et al*., 2012). NF-κB, IL-6 and iNOS play a key role in inflammatory and oxidative injury process activation by triggering the expression of multiple genes of inflammation (Liu *et al*., 2017). In addition, Kim-1 and HO-1 mediate the defense mechanisms of tubular damage and in response to injury the expression level of these proteins are elevated (Zhang and Cai, 2016; Lever *et al*., 2016).

Rutin is a flavonol glycoside comprised of quercetin and the disaccharide rutinose (Sharma *et al*., 2013). Rutin is found in dietary compounds, such as buckwheat, tomato, citrus fruits and apples (Khajuria *et al*., 2019). Studies have demonstrated effective anti-oxidative, anti-allergic, anti-inflammatory and anti-tumor properties for rutin (Rodríguez-García *et al*., 2019). Since, it has both the anti-oxidant and anti-inflammatory properties, it was hypothesized that this compound may protect the rhabdomyolyisis-induced AKI.

In this study, rutin-conjugated gold nanoparticles (Ru-AuNPs) was also synthesized and used at a relatively lesser dose in comparison with the rutin alone. This nano-formulation has the advantages of site-specific drug delivery, improved bioavailability and fewer side effects

*Corresponding author: e-mail: rehan.siddiqui@zu.edu.pk

(Patra *et al*., 2018). Therefore, it was also hypothesized that the results of nano-formulation may be better than the compound alone at low dose which may decrease the risk of side effects.

MATERIALS AND METHODS

Materials and instruments used for the synthesis of Ru-AuNPs

Tetrachloroauric (III) acid trihydrate (99%), rutin trihydrate (94%) and sodium hydroxide (98%) was acquired from Sigma Aldrich. Deionized water was utilized for making all solutions. Shimadzu double beam UV-1800 spectrophotometer having a path length of 1 cm was used for the UV-Visible spectroscopic analysis. Bruker vector 22 FT-IR spectrometer was used to obtain fourier transform infrared (FT-IR) spectrum by using KBr disk method at room temperature between the range of 4000-400 cm-1. Atomic Force Microscope Agilent 5500 was used for the morphological analysis of nanoparticles. Zetasizer Nano ZSP (Malvern) was used to obtain the average particles size and zeta potential of the samples.

Synthesis of rutin coated gold nanoparticles

Rutin coated gold nanoparticles were synthesized using reported method with slight modification (Gul *et al*., 2018). Briefly, Rutin solution (2mg/mL) was prepared in deionized water followed by addition of 50µL of 1 M NaOH. Aqueous gold solution (1mL, 0.5mM) was added dropwise in to the solution of rutin (1mL, 2mg/mL) and magnetically stirred (200 rpm) for 10 minutes at room temperature. When color of the solution changed from yellow to orange, gold solution (1mL, 0.5mM) was added and the color of the solution turned deep red indicating the formation of Ru-AuNPs which was confirmed by UV-visible spectroscopy. Ru-AuNPs were subjected to characterization techniques including FTIR, AFM and DLS for the evaluation of particles size and morphological analysis.

Animals

International guidelines (Institute of Laboratory Animal Resources, US, 1989) and institutional protocols approved by Animal Ethics Committee of Ziauddin University (Approval Protocol No. 2018-002) were implemented during the conduct of the experiments. Male BALB/c mice (average weight 20-30 gm) were acquired from the International Center for Chemical and Biological Sciences, University of Karachi. In their standard cages, animals were kept at 22-23°C with a 12-h light-dark cycle and given free access to rodent chow and water. Before the initiation of the experiment, the animals were habituated with the atmosphere and the experimenter.

Treatment regime

Forty two (42) animals were divided into 7 groups i.e., vehicle control (GP 1), AKI group (GP 2), AKI + rutin 25 mg/kg (GP 3), AKI + rutin 50 mg/kg (GP 4), AKI + Ru-AuNPs 15 mg/kg (GP 5), AKI + Ru-AuNPs 25mg (GP 6), AKI + ascorbic acid 200 mg/kg (GP 7). Animals in GP 1 and GP 2 received normal saline for 4 days while animals in GP 3, and GP 4 were retreated with rutin 25 mg/kg and 50 mg/kg *intraperitoneally* respectively, GP 5 and GP 6 received R Au-NPs 15 mg/kg and 25 mg/kg; and GP 7 acted as positive control which received ascorbic acid 200 mg/kg. On the fourth day, animals of all group were water-deprived for 24 hours followed by *intramuscular* injection of 50% glycerol in the hind limbs at a dose of 10 ml/kg b.w. except for GP 1, which was given normal saline. After 24 hours of glycerol administration, all animals were dissected humanly under general anesthesia for further experiments (Siddiqui *et. al*., 2019).

Serum urea and creatinine analysis

Blood sample was extracted by heart puncture and serum was separated. Serum creatinine and urea were analyzed by Microlab 300 (ELITech Group) to evaluate the kidney functions (Kadir *et. al.*, 2020).

Histopathological examination of kidney tissues

Histological procedures were carried out following standard practice. The tissues were stained with Periodic Acid Schiff's (PAS) and hematoxylin and eosin (H&E) stain and morphological changes were analyzed using Nikon Ts2R-FL inverted microscope. Proximal tubular damage was calculated using Nikon NIS-Elements D software (Kadir *et. al.*, 2020).

Expression Analysis of NFkB p50, iNOS, Kim-1, IL-6 and HO-1 using real-time RT-PCR

Kidney tissues were homogenized and mRNA was isolated using TRIzol method (Life Technologies, USA). cDNA was synthesized using Revert-Aid first-strand cDNA synthesis kit (Fermentas, USA). The primer sequence and protocols for real time RT-PCR studies were followed according the methods described by Siddiqui *et al*. (2019).

STATISTICAL ANALYSIS

Data was analyzed by SPSS version 21. All values are expressed as mean ± SEM. Inter group comparison was done using paired *t*-test followed by one way-ANOVA. *p* value <0.05 was considered statistically significant.

RESULTS

Characterization of rutin coated gold nanoparticles (Ru-AuPNs)

Rutin-coated gold nanoparticles were synthesized by already reported method using slight modification described above. Upon the addition of HAuCl4 solution in to the solution of rutin with constant stirring, appearance of ruby red color indicated the formation of

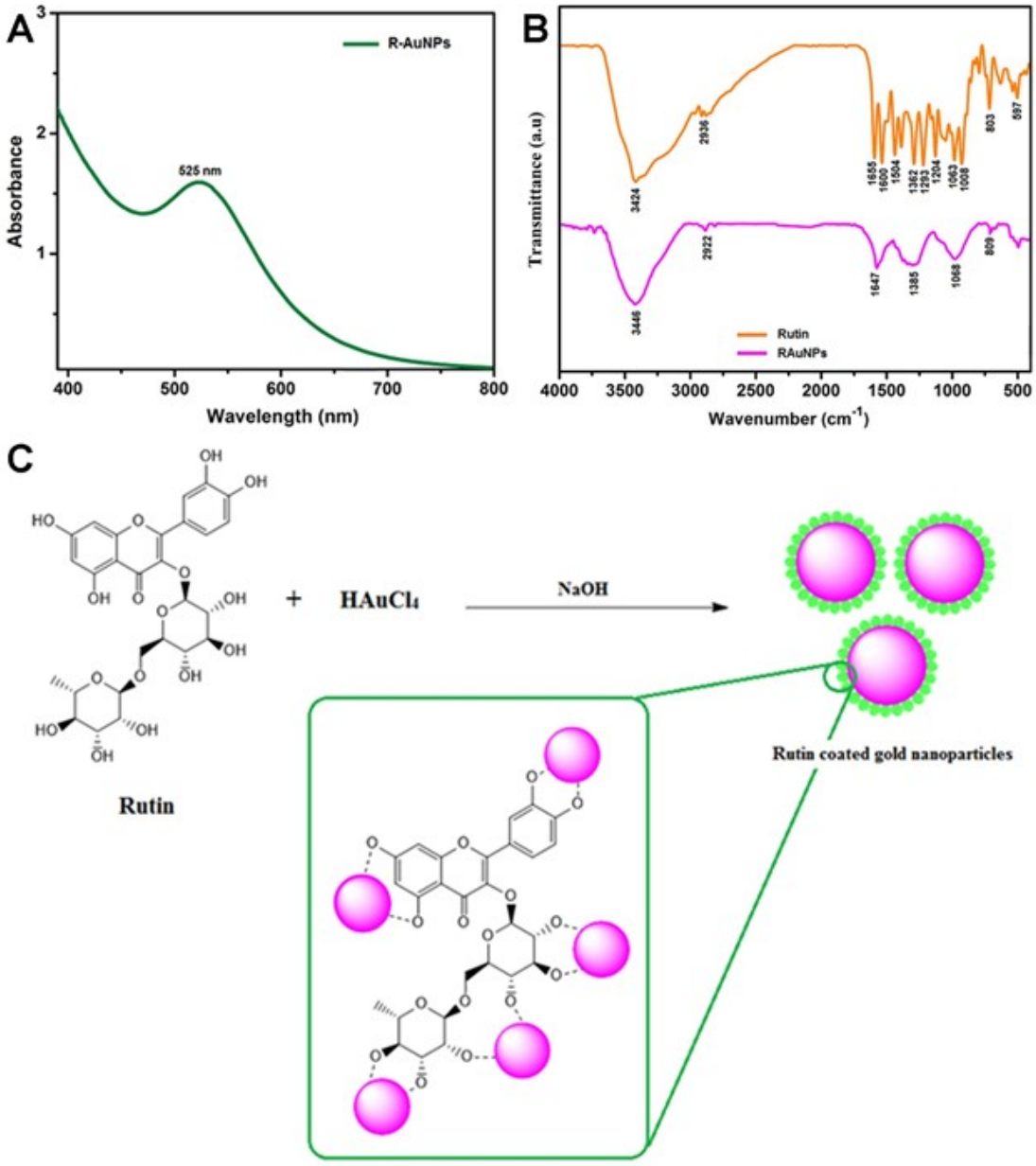

Fig. 1: A. UV-Visible spectrum of rutin coated gold nanoparticles (R-AuNPs). B FTIR analysis of rutin (orange trace) and rutin coated gold nanoparticles (pink trace). C Synthesis of rutin coated gold nanoparticles.

Ru-AuNPs. Upon UV-Visible analysis, Ru-AuNPs exhibited the surface plasmon resonance (SPR) band at 525 nm (Božanić *et al*., 2013) which is given in fig. 1 (A).

Rutin is a plant based flavonoid and it has been reported that flavonoids stabilize gold nanoparticles by the interaction of hydroxyl (-OH) groups which stabilize gold ions (Biao *et al*., 2018). Fig. 1 (C) shows the synthesis of rutin coated gold nanoparticles. FT-IR spectroscopy was employed for the determination of electrostatic interactions of rutin with gold nanoparticles. FT-IR spectra of rutin (orange trace) and rutin coated gold nanoparticles (pink trace) are given in fig. 1 (B). Rutin spectrum showed characteristic absorption peaks of functional groups at 3424 cm-1, 2936 cm-1, 1655 cm-1, 1600 cm-1, 1504 cm-1, 1362 cm-1 and 1063 cm-1. The broad stretching vibrational peak appearing at 3424 cm-1 corresponds to the hydroxyl groups (–OH) present in rutin structure (fig. 1 (B), orange trace). The peaks at 2936 cm-1 and 1655 cm-1 belongs to the stretching frequency of C-H bond and carbonyl group (C=O). Peaks appearing at 1600 cm-1, 1504 cm-1 and 1063 cm−1 are the absorption frequencies of (C=C) alkene, (C=C) aromatic and C-OH bonds. The FT-IR spectrum of Ru-AuNPs showed suppression and shifting of peaks as compared to the rutin spectrum. The major peaks appearing in the spectrum of Ru-AuNPs are at 3446 cm-1, 1647 cm-1, 1385 cm-1 and 1068 cm-1 (fig. 1 (B), pink trace). The peak appearing at

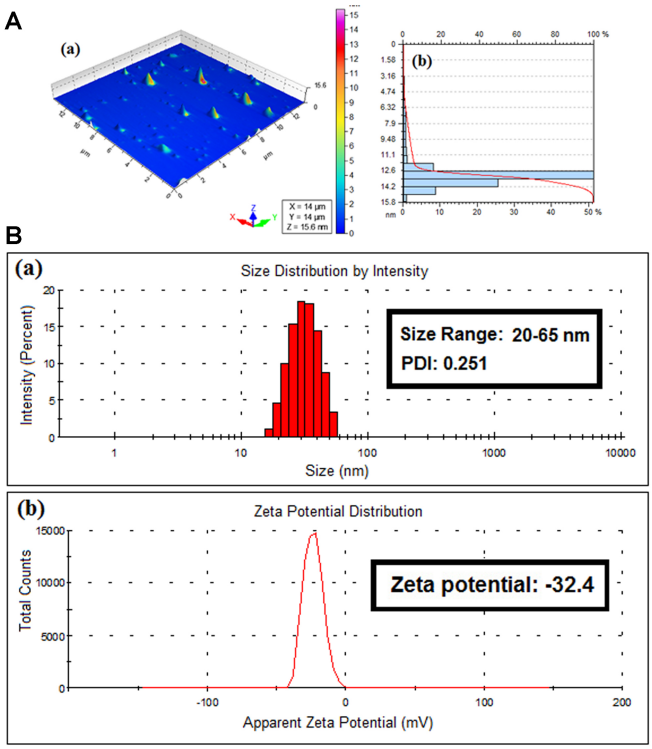

Fig. 2: (A) AFM images of rutin coated gold nanoparticles (a) 3D-height image and (b) average particle height distribution graph. (B) Average particle size distribution histogram of R-AuNPs (a) and zeta potential graph of R-AuNPs (b)

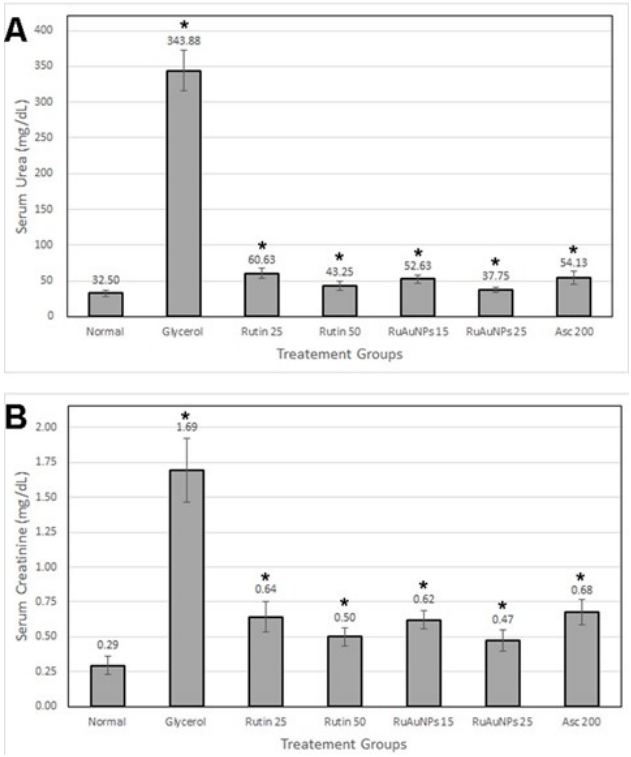

Fig. 3: Serum urea and creatinine levels following rutin and rutin-AuNPs treatment. The levels of serum urea and creatinine were markedly higher in the AKI group as compared to the normal. In comparison with the AKI group it was observed that treatment with rutin and Ru-AuNPs significantly reversed the increase in both biochemical levels. (*p<0.001)

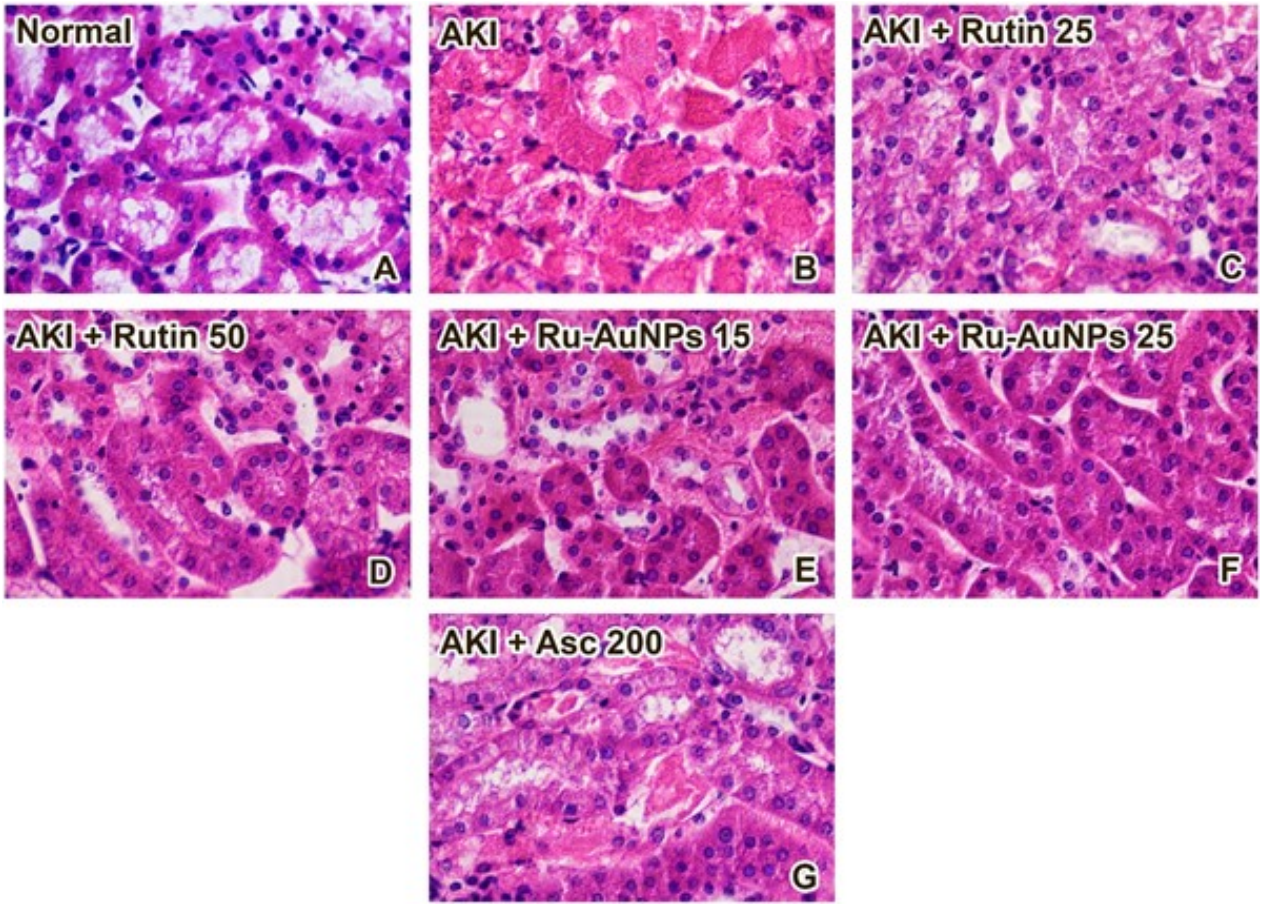

Fig. 4: H&E stained images displaying renal cortex sections. (A) Shows normal kidney cortex. (B) Shows cortex of control AKI sections. (C&D) shows rutin 25 and 50 mg treated group and exhibit decrease in cast deposition and renal tubular damage. (E&F) show rutin-AuNPs 15 and 25 mg treated groups showing significant reduction in renal tubular injury. (G) Shows positive control treated with ascorbic acid 200 mg (Magnification; 400x).

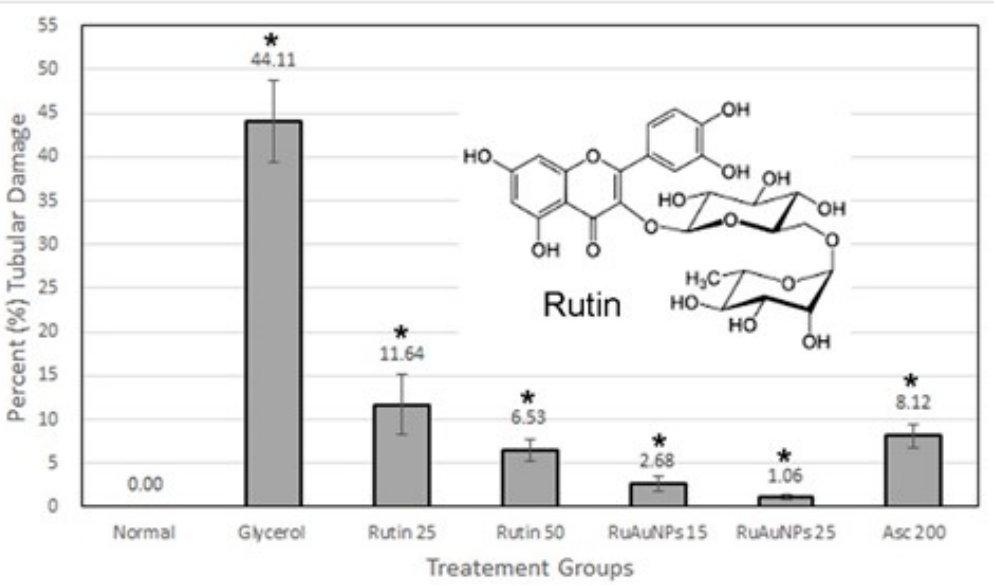

Fig. 5: Damaged area calculation for renal tubules. Marked increase in damaged area in section prepared from control AKI model. Comparing section from AKI control to the treated groups show marked decrease in damage in the treated groups which was maximum in the rutin Au-NPs at low dose (*p<0.001).

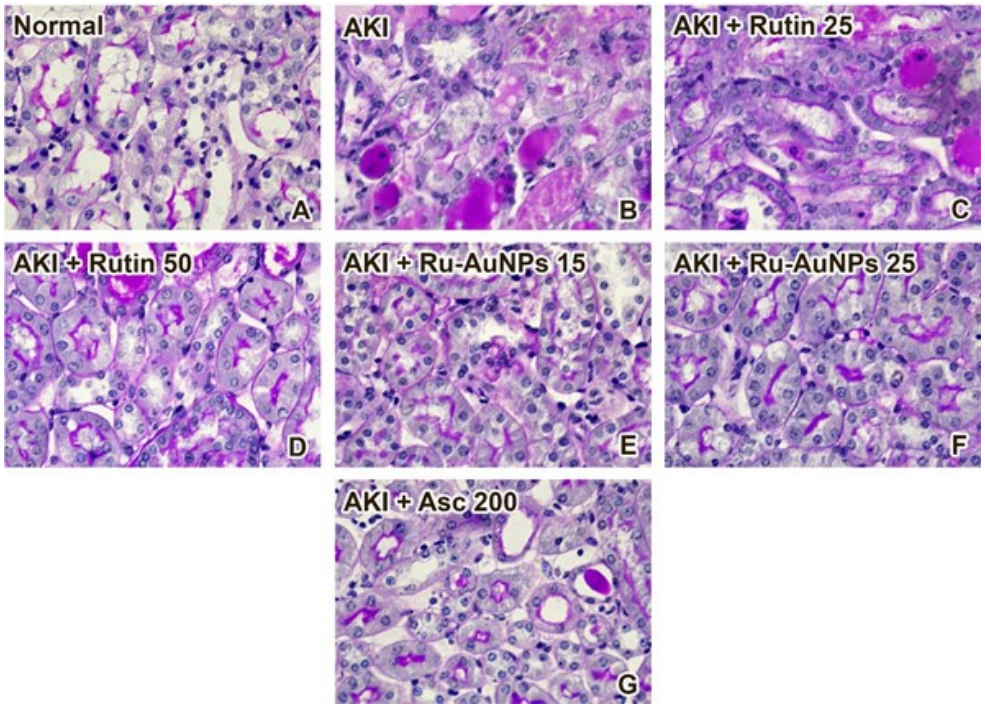

Fig. 6: PAS-stained photomicrograph showing renal cortex sections. (A) Intact kidney brush borders in renal tubules from normal group. (B) Prominent damaged to brush borders of proximal tubules and the loop of Henle cell in AKI group. (C&D) sections from rutin 25 &50mg treated group show decrease in brush border damage. (E&F) rutin-AuNPs 15 & 25 mg treated groups showing marked reduction in damage to brush border and LH cells. (G) ascorbic acid 200 mg treated group (Magnification; 400x).

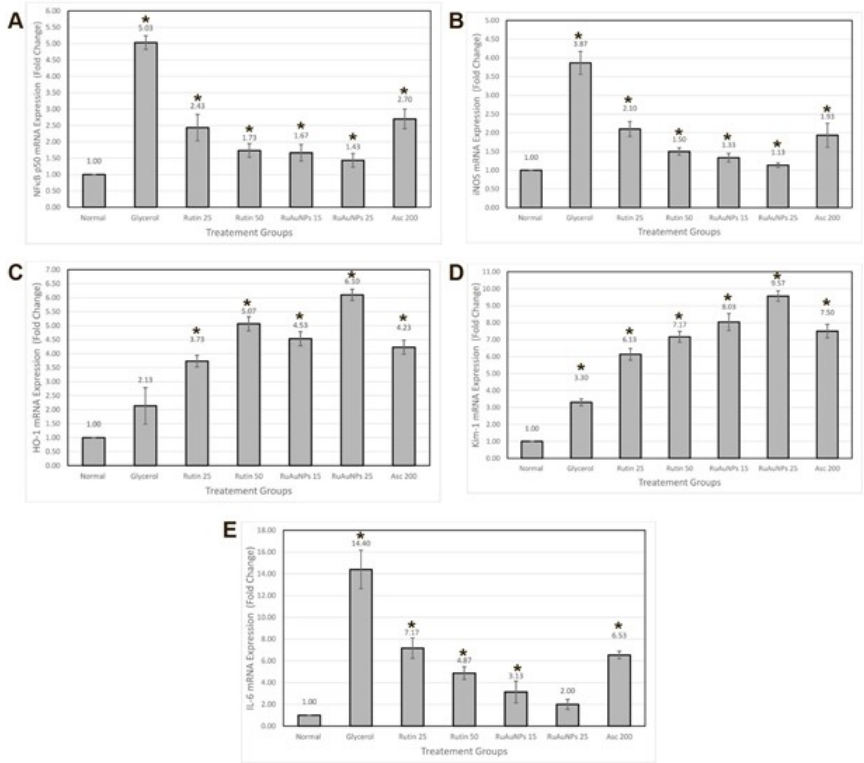

Fig. 7: Effects of rutin and Ru-AuNPs on NF-κB, iNOS, HO-1, Kim-1 and IL-6 mRNA expressions. Rutin and rutin-AuNPs attenuate mRNA expression of NF-κB (A), iNOS (B) and IL-6 (E) while it increases the mRNA expression of HO-1 (C) and Kim-1 (D) (*p<0.001).

3446 cm-1 is the characteristic stretching frequency of the hydroxyl groups (-OH) which is indicating the presence of hydrogen bonding in Ru-AuNPs. The suppression and broadening of peaks at 1647 cm-1 and 1068 cm-1 are indicating the interaction of carbonyl and hydroxyl groups with the gold nanoparticles surface which result in higher stability of Ru-AuNPs (Ateeq *et al*., 2015)

AFM analysis was used for the morphological evaluation of the rutin coated gold nanoparticles as shown in fig. 2 (A, a and b). Fig. 2 (A, a) represents the 3-dimentional height image of Ru-AuNPs. It is evident that nanoparticles have pointed shape and uniform height distribution in the range of 12-14nm. The average particle size distribution of rutin coated gold nanoparticles was determined by using zeta sizer analysis. Fig. 2 (B, a) shows the histogram of average particle size of Ru-AuNPs, which are in the range of 20-65 nm. Polydispersity index (PDI) of Ru-AuNPs was found to be 0.251, indicating the formation of nanoparticles having highly uniform size distribution. Zeta potential analysis was carried out for the evaluation of surface charges over R-AuNPs and its graph is given in fig. 2 (B, b). The graph indicated that the magnitude of surface charges over Ru-AuNPs is -32.4 mV. The higher value of zeta potential of Ru-AuNPs, corresponds to higher stability and less aggregation of nanoparticles.

Rutin and rutin-AuNPs reduce serum urea and creatinine level

A notable rise was observed in serum levels of creatinine and urea of the AKI group compared to the normal control (p<0.001). However, rutin and Ru-AuNPs administration considerably lowered both parameters (p <0.001) in comparison with the AKI group (fig. 3).

Rutin and Ru-AuNPs inhibit cast deposition and proximal tubular necrosis

Fig. 4 shows classic kidney H&E staining. Noticeable necrosis and inflammation of proximal tubules were seen in the glycerol-treated animals along with protein casts deposition and damage to cells of LH. On the other hand, significant proximal tubular damage inhibition and reduced deposition of pathological protein casts in tubules were observed in animals pretreated with rutin (25 and 50 mg/kg). Animals pretreated with rutin-AuNPs (15 and 25 mg/kg) showed approximate complete protection against kidney injury. Measuring tubular damage revealed 44% damage in the AKI group as compared to the normal group (p<0.001). On the other hand, there was only 11% and 6% damage in kidneys pretreated with rutin 25 mg and 50 mg. This improvement in damage was further enhanced to 2% and 1% (p<0.001) with rutin AuNPs of 15 mg and 25mg respectively. The positive control treated with Asc 200mg showed a damage of 8% (fig. 5).

Rutin and Ru-AuNPs conserve brush borders of PCT and LH

PAS stained kidney is shown in fig. 6. There is an almost complete destruction of the brush border in the AKI group, whereas the groups pretreated with rutin 25mg and 50 mg show a decrease in damage to the brush borders. However, there was an almost complete restoration of the brush border in the groups pretreated with rutin-AuNPs 15mg and 25mg. Both rutin and Ru-AuNPs were superior to ascorbic acid a known compound which only partially protected the renal tubule.

Rutin and rutin-AuNPs down-regulate the mRNA expressions of iNOS, IL-6 and NFκB p50 genes, and upregulate HO-1 and Kim-1

Fig. 7 shows the real-time RT-PCR data for iNOS, IL-6, NFkB p50, Kim-1 and HO-1. iNOS, IL-6 and NFkB p50 fig 6 A, B &E were increased significantly in the glycerol treated group in comparison with the normal group (p <0.001). However, they were reduced in the rutin and Ru-AuNPs treated groups (p<0.001). No notable change in the HO-1 and Kim-1 is observed in AKI group compared to the normal control however the expression increased exponentially in the rutin (p<0.001) and Ru-AuNPs (p<0.001) treated groups.

DISCUSSION

In the present study we evaluated the anti-inflammatory and anti-oxidative activities of rutin on rhabdomyolysis-induced AKI. Many of the murine models researching AKI are based on nephrotoxic drug injection and/or administration, such as gentamicin, cisplatin etc. (Holditch *et al*., 2019; Medic *et al*., 2019). Nevertheless, none of these above mentioned animal models imitate the precise patho-morphology of AKI as occurring in rhabdomyolysis. The nearest mechanisms of AKI in animals can only be induced by glycerol.

Glycerol essentially causes muscle damage due to release of myoglobin into the bloodstream which induces hemolysis, as a result of release of hemoglobin into the blood. Metallic catalytic iron center is present in both myoglobin and hemoglobin. When these heme containing proteins pass through the kidneys, the catalytic iron is the reason for lipid peroxidation of the kidney tubules with resultant oxidative stress, inflammation, cast formation and apoptosis causing tubular obstruction (Zorova *et al*., 2016). Therefore, this murine model was selected to study the protective activity of rutin and Ru-AuNPs against AKI.

The current study explicated the preventive effects of rutin and Ru-AuNPs and revealed that rhabdomyolysis-induced AKI in mice was perfectly prevented by this compound. Rutin and Ru-AuNPs also prevented renal tubular damage and reduced the blood levels of creatinine and urea.

Drug delivery, bioavailability and adverse effects are important as well as limiting factors in medicine. Kidneys are the crucial part of the body for excretion and for this reason they are the main organ for drug toxicity (Faria *et al*., 2019). Incorporation of nanoparticles with different drug has the advantage of reducing the drawbacks of drug availability and adverse effects (Rizvi and Saleh, 2018). Therefore, we integrated rutin with its gold nanoparticles with added advantage of decrease dose of the required compound. We also explored the possible underlying mechanisms of tubular protection by rutin and its gold nanoparticles by iNOS, KIM-1, NF-κB p50, IL-6 and HO-1 in animal model of AKI.

NF-κB is a pleiotropic protein with distinct features (Zhang *et al*., 2017). It plays a vital role in cell survival and cytokine production (Taniguchi and Karin, 2018). Primarily NF-κB controls the degree and duration of inflammatory reactions by several mechanisms (Liu *et al*., 2017). The outcomes of this study manifest increased levels of NF-κB p50 in group treated with glycerol in comparison with the normal control. However, rutin and Ru-AuNPs greatly down-regulated the mRNA expression of NF-κB p50. NF-κB triggers the iNOS gene expression which is responsible for induction of inflammation (Jiang *et al*., 2018; Ha *et al*., 2016) Likewise iNOS is involved in the control of inflammatory cytokine such as NO (Xue *et al*., 2018). In our study we also observed a significant rise in mRNA expression of iNOS in animal groups treated with glycerol. However, in rutin and rutin AuNPs treated group the expression of iNOS was downregulated significantly. This demonstrates that high oxidative state in glycerol treated animals is adversely moderated by the treatment of rutin and Ru-AuNPs.

The iNOS-induced NO causes induction of heme oxygenase-1 (HO-1) enzyme, responsible for the catabolism of heme to biliverdin, iron and carbon monoxide as by products (Rochette *et al*., 2018; Ryter and Choi, 2016). Stress also induces HO-1 and in this situation it has immunomodulatory and anti-inflammatory functions (Ryter and Choi, 2016). Therefore, it plays a vital role in modulation of inflammation by up regulating interleukin-1R antagonist and interleukin-10 expression (Siddiqui *et al*., 2019; Ebersole *et al*., 2017). In our study it is found to be significantly raised in rutin and Ru-AuNPs treated groups as compared to AKI group and normal controls.

A recently identified molecule for characterization of tubular injury is Kim-1. Kim-1 expression is increased in inflammatory conditions (Beker *et al*., 2018; McWilliam *et al*., 2018). In our study we found the expression of KIM-1 to increase in rutin and Ru-AuNPs treated groups as compared to normal controls which was in agreement with previous studies.

CONCLUSION

Rutin protects against rhabdomyolysis-induced AKI by decreasing levels of creatinine and urea. Gold nanoparticle conjugates of rutin (Ru-AuNPs) conserve kidney structure at a lower dose as compared to rutin alone. Rutin and its gold nano formulation effectively preserve kidney tubular structure. The mechanism of protection appears to be the down regulation of IL-6 gene therefore protecting from oxidant injury and inflammation. Rutin also up-regulate the mRNA expressions of KIM-1 and HO-1 and down-regulate the expressions of NF-κB and iNOS. We hope that this compound will open new doors for future research and clinical trials.

ACKNOWLEDGMENT

The authors thank to Ziauddin University for providing the research laboratories facility to carry out the presented research work.

REFERENCES

Abd-Ellatif RN, Hegab II, Atef MM, Sadek MT and Hafez YM (2019). Diacerein protects against glycerol-induced acute kidney injury: modulating oxidative stress, inflammation, apoptosis and necroptosis. *Chem-Biol. Interact.*, **306**: 47-53.

Ateeq M, Shah MR, ul Ain N, Bano S, Anis I, Faizi S, Bertino MF and Naz SS (2015). Green synthesis and molecular recognition ability of patuletin coated gold nanoparticles. *Biosens. Bioelectron*., **63**: 499-505.

Beker BM, Corleto MG, Fieiras C and Musso CG (2018). Novel acute kidney injury biomarkers: Their characteristics, utility and concerns. *Int. Neurol. Nephrol.*, **50**(4): 705-713.

Biao L, Tan S, Meng Q, Gao J, Zhang X, Liu Z and Fu Y (2018). Green synthesis, characterization and application of proanthocyanidins-functionalized gold nanoparticles. *Nanomater*., **8**(1): 53.

Božanić DK, Luyt AS, Trandafilovic LV and Djokovic V (2013). Glycogen and gold nanoparticle bioconjugates: controlled plasmon resonance via glycogen-induced nanoparticle aggregation. *RSC Adv*., **3**(23): 8705-8713.

Cui,J, Tang L, Hong Q, Lin S, Sun X, Cai G, Bai XY and Chen X (2019). N-acetylcysteine ameliorates gentamicin-induced nephrotoxicity by enhancing autophagy and reducing oxidative damage in miniature pigs. *Shock*, **52**(6): 622.

Ebersole JL, Dawson III D, Emecen Huja P, Nagarajan R, Howard K, Grady ME, Thompson K, Peyyala R, Al-Attar A, Lethbridge K and Kirakodu S (2017). The periodontal war: microbes and immunity. *Periodontol*, **75**(1): 52-115.

El-Kordy EA (2019). Effect of suramin on renal proximal tubular cells damage induced by cisplatin in rats

(histological and immunohistochemical study). *J. Microsc. Ultrastruct*., **7**(4): 153.

Faria J, Ahmed S, Gerritsen KG, Mihaila SM and Masereeuw R (2019). Kidney-based in vitro models for drug-induced toxicity testing. *Arch. Toxicol.*, **93**: 3397-3418.

Gao J, Gu Z, Li M, Xu Y, Gao Y, Wei J, Liang B and Na Y (2017). L-Carnitine Ameliorates the Decrease of Aquaporin 2 Levels in Rats with Cisplatin-Induced Kidney Injury. *Nephron*, **135**(4): 315-325.

Gul A, Kunwar B, Mazhar M, Faizi S, Ahmed D, Shah MR and Simjee SU (2018). Rutin and rutin-conjugated gold nanoparticles ameliorate collagen-induced arthritis in rats through inhibition of NF-κB and iNOS activation. *Int. Immunopharmacol*., **59**: 310-317.

Ha SK, Sung J, Choi I and Kim Y (2016). Oryza sativa (Rice) hull extract inhibits lipopolysaccharide-induced inflammatory response in RAW264. 7 macrophages by suppressing extracellular signal-regulated kinase, c-jun n-terminal kinase and nuclear factor-κb activation. *Pharmacog. Mag*., **12**(48): 295.

Holditch SJ, Brown CN, Lombardi AM, Nguyen KN and Edelstein CL (2019). Recent advances in models, mechanisms, biomarkers and interventions in cisplatin-induced acute kidney injury. *Int. J. Mol. Sci*., **20**(12): 3011.

Institute of Laboratory Animal Resources (US). Committee on Care and Use of Laboratory Animals. (1986). Guide for the care and use of laboratory animals (No.86). US Department of Health and Human Services, Public Health Service, National Institutes of Health, The National Academies Press, NW Washington, DC, USA.

Jiang Y, Liu J, Zhou Z, Liu K and Liu C (2018). Diosmetin attenuates Akt signaling pathway by modulating nuclear factor kappa-light-chain-enhancer of activated B cells (NF-κB)/inducible nitric oxide synthase (iNOS) in streptozotocin (STZ)-induced diabetic nephropathy mice. Medical science monitor: *Int. Med. J. Exp. Clin. Res.*, **24**: 7007.

Kadir A, Sher S, Siddiqui RA and Mirza T (2020). Nephroprotective role of eugenol against cisplatin-induced acute kidney injury in mice. *Pak. J. Pharm. Sci.*, **33**(3): 1281-1287.

Khajuria R, Singh S and Bahl A (2019). General introduction and sources of flavonoids. in current aspects of Flavonoids: Their role in cancer treatment. *Springer*, Singapore, pp.1-7.

Kher V, Srisawat N, Noiri E, Gharbi MB, Shetty MS, Yang L, Bagga A, Chakravarthi R, Mehta R, Group C and Acute Disease Quality Initiative (2017). Prevention and therapy of acute kidney injury in the developing world. *Kid. Int. Rep*., **2**(4): 544-558.

Korrapati MC, Shaner BE and Schnellmann RG (2012). Recovery from glycerol-induced acute kidney injury is accelerated by suramin. *J. Pharmacol. Exp. Ther*., **341**(1): 126-136.

Lever JM, Boddu R, George JF and Agarwal A (2016). Heme oxygenase-1 in kidney health and disease. *Antioxid. Redox Sign*., **25**(3): 165-183.

Li W, Li D, Xu T, Zhang Y, Zhu H and Han F (2011). Prevention of contrast-induced acute kidney injury with ascorbic acid and prostaglandin E1 in high risk factors patients undergoing PCI. *Heart*, **97**(3): A151-A151.

Liu T, Zhang L, Joo D and Sun SC (2017). NF-κB signaling in inflammation. *Signal Transduct. Tar*., **2**(1): 1-9.

Makris K and Spanou L (2016). Acute kidney injury: definition, pathophysiology and clinical phenotypes. The *Clin. Biochem. Rev*., **37**(2): 85.

Manis T, George-Varghese B and Kashani J (2019). Rhabdomyolysis-Go big or go home. *Am. J. Emerg. Med*., **37**(12): 2194-2196.

McWilliam SJ, Antoine DJ, Jorgensen AL, Smyth RL and Pirmohamed M (2018). Urinary biomarkers of aminoglycoside-induced nephrotoxicity in cystic fibrosis: kidney injury molecule-1 and neutrophil gelatinase-associated lipocalin. *Sci. Rep*., **8**(1): 1-9.

Medić B, Stojanović M, Rovčanin B, Kekic D, Skodric SR, Jovanović GB, Vujović KS, Divac N, Stojanović R, Radenković M and Prostran M (2019). Pioglitazone attenuates kidney injury in an experimental model of gentamicin-induced nephrotoxicity in rats. *Sci. Rep*., **9**(1): 1-10.

Ozturk O, Ustebay S, Eroglu HA, Gunay M, Adali Y, Donmez İ and Erbas M (2017). An experimental study of ascorbic acid effects in acute renal failure under general anesthesia. *Acta Cir. Bras*., **32**(10): 853-861.

Patra JK, Das G, Fraceto LF, Campos EVR, del Pilar Rodriguez-Torres M, Acosta-Torres LS, Diaz-Torres L.A, Grillo R, Swamy MK, Sharma S and Habtemariam S (2018). Nano based drug delivery systems: recent developments and future prospects. *J. Nanobiotechnol*., **16**(1): 71.

Petejova N, Martinek A and Zadrazil J (2018). Acute kidney injury due to rhabdomyolysis. *Adv. Med. Biol*., **135**: 1-269.

Rizvi SA and Saleh AM (2018). Applications of nanoparticle systems in drug delivery technology. *Saudi Pharm. J*., **26**(1): 64-70.

Rochette L, Zeller M, Cottin Y and Vergely C (2018). Redox functions of heme oxygenase-1 and biliverdin reductase in diabetes. *Trends Endocrin. Met*., **29**(2): 74-85.

Rodríguez-García C, Sánchez-Quesada C and Gaforio JJ (2019). Dietary flavonoids as cancer chemopreventive agents: An updated review of human studies. *Antiox*., **8**(5): 137.

Ryter SW and Choi AM (2016). Targeting heme oxygenase-1 and carbon monoxide for therapeutic modulation of inflammation. *Trans. Res*., **167**(1): 7-34.

Sharma S, Ali A, Ali J, Sahni JK and Baboota S (2013). Rutin: therapeutic potential and recent advances in

drug delivery. *Expert Opin. Inv. Drug*., **22**(8): 1063-1079.

Siddiqui RA, Simjee SU, Kabir N, Ateeq M, Shah MR and Hussain SS (2019). N-(2-hydroxyphenyl) acetamide and its gold nanoparticle conjugation prevent glycerol-induced acute kidney injury by attenuating inflammation and oxidative injury in mice. *Mol. Cell Biochem*., **450**(1-2): 43-52.

Taniguchi K and Karin M (2018). NF-κB, inflammation, immunity and cancer: Coming of age. *Nat. Rev. Immunol*., **18**(5): 309-324.

Xue Q, Yan Y, Zhang R and Xiong H (2018). Regulation of iNOS on immune cells and its role in diseases. *Int. J. Mol. Sci*., **19**(12): 3805.

Zhang Q, Lenardo MJ and Baltimore D (2017). 30 years of NF-κB: A blossoming of relevance to human pathobiology. *Cell*, **168**(1-2): 37-57.

Zhang Z and Cai CX (2016). Kidney injury molecule-1 (KIM-1) mediates renal epithelial cell repair via ERK MAPK signaling pathway. *Mol. Cell Biochem*., **416**(1-2): 109-116.

Zorova LD, Pevzner IB, Chupyrkina AA, Zorov SD, Silachev DN, Plotnikov EY and Zorov DB (2016). The role of myoglobin degradation in nephrotoxicity after rhabdomyolysis. *Chem Biol. Interact*., **256**: 64-70.